

# PROCEEDINGS OF SPIE

[SPIDigitalLibrary.org/conference-proceedings-of-spie](https://spiedigitallibrary.org/conference-proceedings-of-spie)

## Three-dimensional deep tissue multiphoton frequency-domain fluorescence lifetime imaging microscopy via phase multiplexing and adaptive optics

Yide Zhang, Ian H. Guldner, Evan L. Nichols, David Benirschke, Cody J. Smith, et al.

Yide Zhang, Ian H. Guldner, Evan L. Nichols, David Benirschke, Cody J. Smith, Siyuan Zhang, Scott S. Howard, "Three-dimensional deep tissue multiphoton frequency-domain fluorescence lifetime imaging microscopy via phase multiplexing and adaptive optics," Proc. SPIE 10882, Multiphoton Microscopy in the Biomedical Sciences XIX, 108822H (22 February 2019); doi: 10.1117/12.2510674

**SPIE.**

Event: SPIE BiOS, 2019, San Francisco, California, United States

# Three-dimensional deep tissue multiphoton frequency-domain fluorescence lifetime imaging microscopy via phase multiplexing and adaptive optics

Yide Zhang<sup>1,\*</sup>, Ian H. Guldner<sup>2</sup>, Evan L. Nichols<sup>2</sup>, David Benirschke<sup>1</sup>, Cody J. Smith<sup>2</sup>, Siyuan Zhang<sup>2</sup>, and Scott S. Howard<sup>1</sup>

<sup>1</sup>Department of Electrical Engineering, University of Notre Dame, Notre Dame, IN 46556, USA

<sup>2</sup>Department of Biological Sciences, University of Notre Dame, Notre Dame, IN 46556, USA

## ABSTRACT

We propose and demonstrate a novel multiphoton frequency-domain fluorescence lifetime imaging microscopy (MPM-FD-FLIM) system that is able to generate 3D lifetime images in deep scattering tissues. The imaging speed of FD-FLIM is improved using phase multiplexing, where the fluorescence signal is split and mixed with the reference signal from the laser in a multiplexing manner. The system allows for easy generation of phasor plots, which not only address multi-exponential decay problems but also clearly represent the dynamics of the fluorophores being investigated. Lastly, a sensorless adaptive optics setup is used for FLIM imaging in deep scattering tissues. The capability of the system is demonstrated in fixed and living animal models, including mice and zebrafish.

**Keywords:** Fluorescence lifetime imaging microscopy, frequency-domain, multiphoton microscopy, adaptive optics, in vivo imaging, deep tissue imaging, radio frequency, multiplexing

## 1. INTRODUCTION

Fluorescence lifetime imaging microscopy (FLIM) is a useful tool for biomedical research because it provides additional information other than fluorescence intensity, such as ion concentration, dissolved oxygen concentration, pH, and refractive index by measuring the fluorescence decay lifetime of excited fluorophores.<sup>1-3</sup> FLIM becomes especially powerful when combined with multiphoton microscopy (MPM)<sup>4-8</sup> which provides 3D resolution, deep penetration, and minimal phototoxicity.<sup>9-11</sup> FLIM can be implemented in time-domain (TD)<sup>12,13</sup> or frequency-domain (FD).<sup>14,15</sup> FD-FLIM techniques are attractive for their rapid acquisition speed, easy implementation, and reduced system bandwidth requirements compared to TD-FLIM.<sup>1</sup> However, both TD- and FD-FLIM techniques are slow compared to a conventional confocal or multiphoton microscopy due to the extra data acquisition and processing steps required to acquire fluorescence lifetime information. Moreover, FLIM images often suffer from their low signal-to-noise ratio (SNR) because the photon efficiency in measuring fluorescence lifetimes is low compared to conventional intensity measurements;<sup>1,16</sup> this problem is more prominent in deep tissue imaging, where useful ballistic photons are scarce and FLIM imaging is particularly challenging. The slow speed and low SNR are thus the main factors that limit FLIM from being widely used in biomedical research.

In this work, we propose and demonstrate a novel multiphoton FD-FLIM (MPM-FD-FLIM) system that is able to generate three-dimensional (3D) lifetime images in deep scattering tissues. The imaging speed of FD-FLIM is improved using a radio frequency (RF) analog signal processing technique termed phase multiplexing, where the multiphoton excitation fluorescence signal is split to multiple ways, phase shifted, and mixed with the 80 MHz reference signal from a Ti:sapphire laser in a multiplexing manner. This technique is fundamentally a homodyne detection method aiming to extract the fundamental harmonic of the 80 MHz pulses, but no external modulation is used and therefore the photon efficiency is high. Moreover, due to the multiplexing and analog signal processing, 3D fluorescence lifetime and intensity images can be acquired simultaneously, with no additional time required for FD-FLIM measurements. We also show that this system allows for easy generation of phasor plots with no Fourier transform involved, which not only address multi-exponential fluorescence decay problems

---

\*e-mail: yzhang34@nd.edu

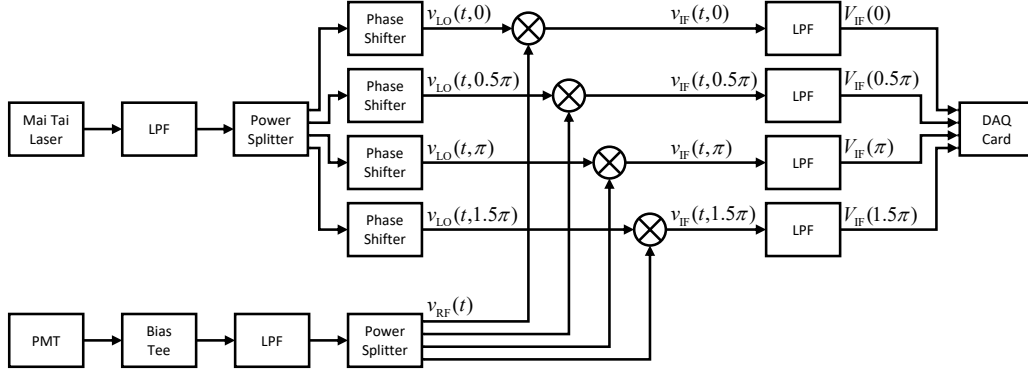


Figure 1. Schematic of a PM-FLIM system.

but also clearly represent the dynamics of the fluorophores being investigated. A custom-written program allows one to interact with fluorophore dynamics by selecting a certain area of phasor plots and observing the image pixels related to it. Lastly, a sensorless adaptive optics setup with a deformable mirror is used in the system to correct wavefront distortions introduced by the imaging system and sample and allows for FLIM imaging in deep scattering tissues. The capability of the system is demonstrated in fixed and living animal models, including mice and zebrafish.

## 2. METHODS

The phase multiplexing (PM) FLIM system is an upgrade of the generalized stepwise optical saturation (GSOS) microscope we developed to acquire super-resolution FD-FLIM images.<sup>17</sup> In Ref. 17, we used analog RF mixing to extract the fundamental harmonic component,  $q_1$ , by measuring the voltage at the intermediate frequency (IF) port of the RF mixer (Mini-Circuits ZAD-3H+, 0.05-200 MHz) four times, each time with a different phase shift introduced by a phase shifter (Mini-Circuits JSPHS-150+, 100-150 MHz). After acquiring these four measurements,  $V_{IF}(0)$ ,  $V_{IF}(0.5\pi)$ ,  $V_{IF}(\pi)$ ,  $V_{IF}(1.5\pi)$ , we can calculate the phase of the harmonic  $q_1$  from

$$\angle q_1 = \arctan \left[ \frac{V_{IF}(\pi) - V_{IF}(0)}{V_{IF}(0.5\pi) - V_{IF}(1.5\pi)} \right], \quad (1)$$

and the fluorescence lifetime  $\tau$  can be calculated as

$$\tau = -\frac{1}{\omega} \tan(\angle q_1) = \frac{1}{\omega} \frac{V_{IF}(0) - V_{IF}(\pi)}{V_{IF}(0.5\pi) - V_{IF}(1.5\pi)}. \quad (2)$$

The four measurements also allow for easy generation of phasor plots<sup>18-20</sup> with no Fourier transform involved,

$$V_{IF}(0) - V_{IF}(\pi) \propto S, \quad (3)$$

$$V_{IF}(0.5\pi) - V_{IF}(1.5\pi) \propto G, \quad (4)$$

where  $S$  and  $G$  are imaginary and real coordinates of a point in a phasor plot. The phasor plots not only address multi-exponential fluorescence decay problems but also clearly represent the dynamics of the fluorophores being investigated.

In this work, we upgraded the GSOS design by introducing two power splitters (Mini-Circuits ZSC-4-3+, 0.25-250 MHz) as well as three additional phase shifters, RF mixers, and low-pass filters into the experimental setup, as shown in Fig. 1. The two power splitters are able to split the signals from the mode-locked Ti:sapphire laser (Spectra Physics Mai Tai BB, 710-990 nm, 100 fs, 80 MHz) and the PMT (Hamamatsu H7422PA-40) to four paths. The four paths are independent and each one of them can be seen as a replica of the analog RF mixing configuration in Ref. 17. The analog RF mixing can be operated simultaneously by introducing four different phases, 0,  $0.5\pi$ ,  $\pi$ ,  $1.5\pi$ , to the phase shifter at each path; therefore one no longer needs to repeat

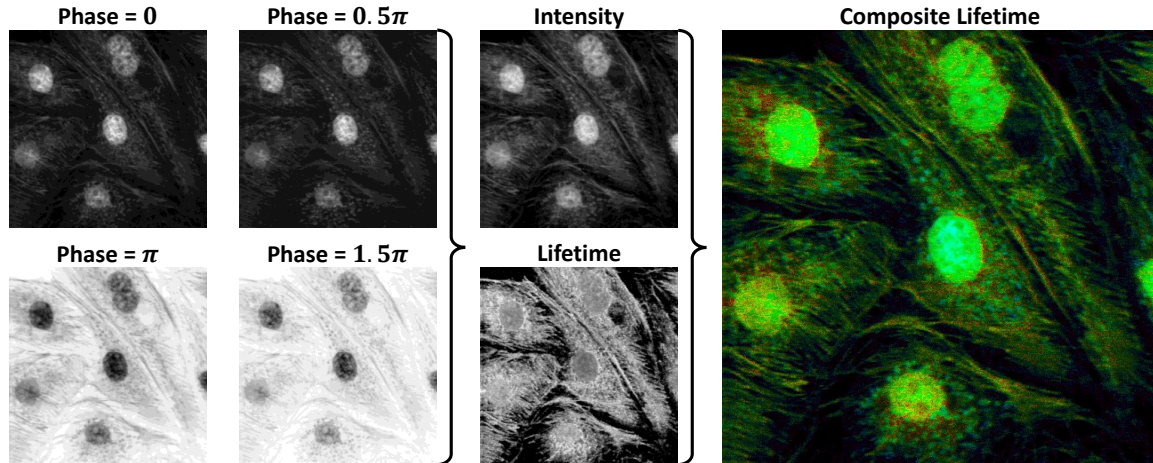


Figure 2. In PM-FLIM, the four measurements (with different phase shifts) required to calculate the fluorescence lifetime image can be acquired simultaneously. With the intensity image measured at the same speed, a composite lifetime image can be generated, where the intensity and lifetime are mapped to each pixel's brightness and hue, respectively. Shown here are images from fixed bovine pulmonary artery endothelial (BPAE) cells (Invitrogen FluoCells F36924) labeled with MitoTracker Red CMXRos (mitochondria), Alexa Fluor 488 phalloidin (F-actin), and DAPI (nuclei).

the measurement four times as we did in Ref. 17. Instead, all the four measurements required to acquire the fluorescence lifetime  $\tau$  can be performed simultaneously, in a multiplexing manner; hence we call this technique phase multiplexing FLIM. The PM-FLIM technique not only makes FLIM imaging four times faster than our previous setup, it also generates lifetime images and phasor plots at the same speed with a conventional confocal or multiphoton microscope. Therefore, with PM-FLIM, the low speed is no longer a limiting factor of FLIM. The principle of PM-FLIM can be seen from an example in Fig. 2.

With the capability to generate fluorescence lifetime images and phasor plots at the same speed with conventional confocal or multiphoton intensity images, PM-FLIM enables the opportunities to get 3D lifetime images and phasor plots in deep scattering tissues. We utilized a piezoelectric deformable mirror (Thorlabs DMP40) to compensate for the optical aberration of the beam when imaging deep. We used a sensorless adaptive optics (AO) technique similar to the one in Ref. 21 to compensate for wavefront distortions. With the combination of PM-FLIM and AO, we achieved 3D *in vivo* fluorescence lifetime imaging in live mouse brain and zebrafish embryo. All animal studies in this work were approved by the University of Notre Dame Institutional Animal Care and Use Committee.

### 3. RESULTS

We performed a series of imaging experiments with our PM-FLIM setup. For each experiment,  $G$  and  $S$  images were calculated from the four multiplexing measurements,  $V_{IF}(0)$ ,  $V_{IF}(0.5\pi)$ ,  $V_{IF}(\pi)$ ,  $V_{IF}(1.5\pi)$ , based on Eqs. 3 and 4. Intensity images were obtained in a conventional manner, i.e., by recording the DC component of the fluorescence signal detected by the PMT; in practice, we measured the DC port of the bias tee to acquire intensity information. Lifetime images were obtained with Eq. 2. Composite lifetime images were generated by mapping the intensity and lifetime images to the pixels' brightness and hue, respectively. Phasor plots were in principle two-dimensional histograms of  $G$  and  $S$  images. By drawing region-of-interests (ROIs) on phasor plots using our custom-written program, the pixels related to the ROIs could be labeled; consequently, a phasor labeling image could be generated, where the pixels corresponding to the aforementioned ROIs were painted with the same color as their related ROIs. With the new phasor labeling image, a composite phasor image with brightness mapped to intensity and hue mapped to phasor labels could also be generated. Lastly, we applied a  $3 \times 3$  median filter to  $G$  and  $S$  images to improve the SNR performance of the phasor plot.<sup>20</sup> After filtering, the phasor plots became more congregated and the accuracy of phasor labeling was increased.

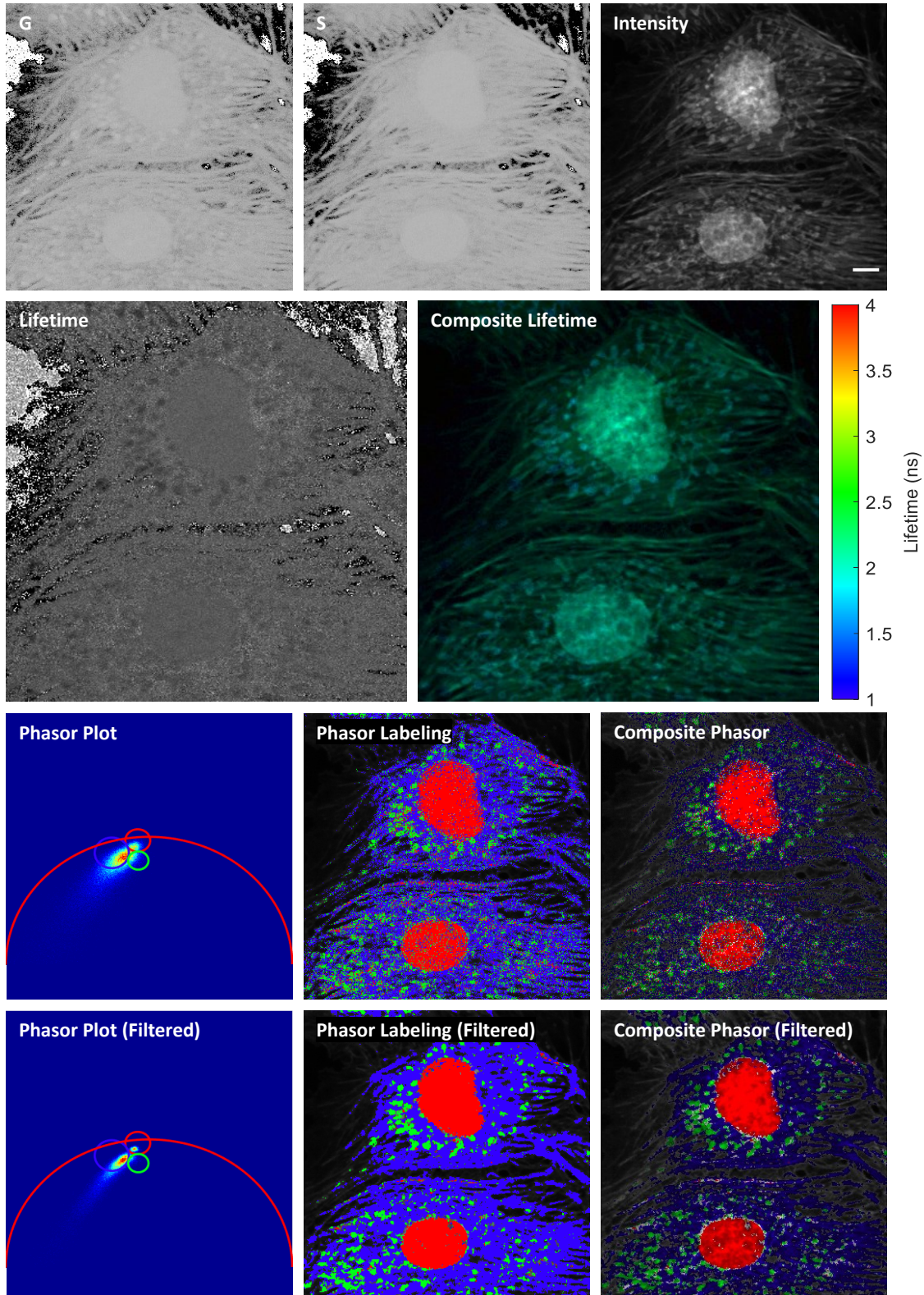


Figure 3. Images of fixed BPAE cells acquired with a PM-FLIM microscope.

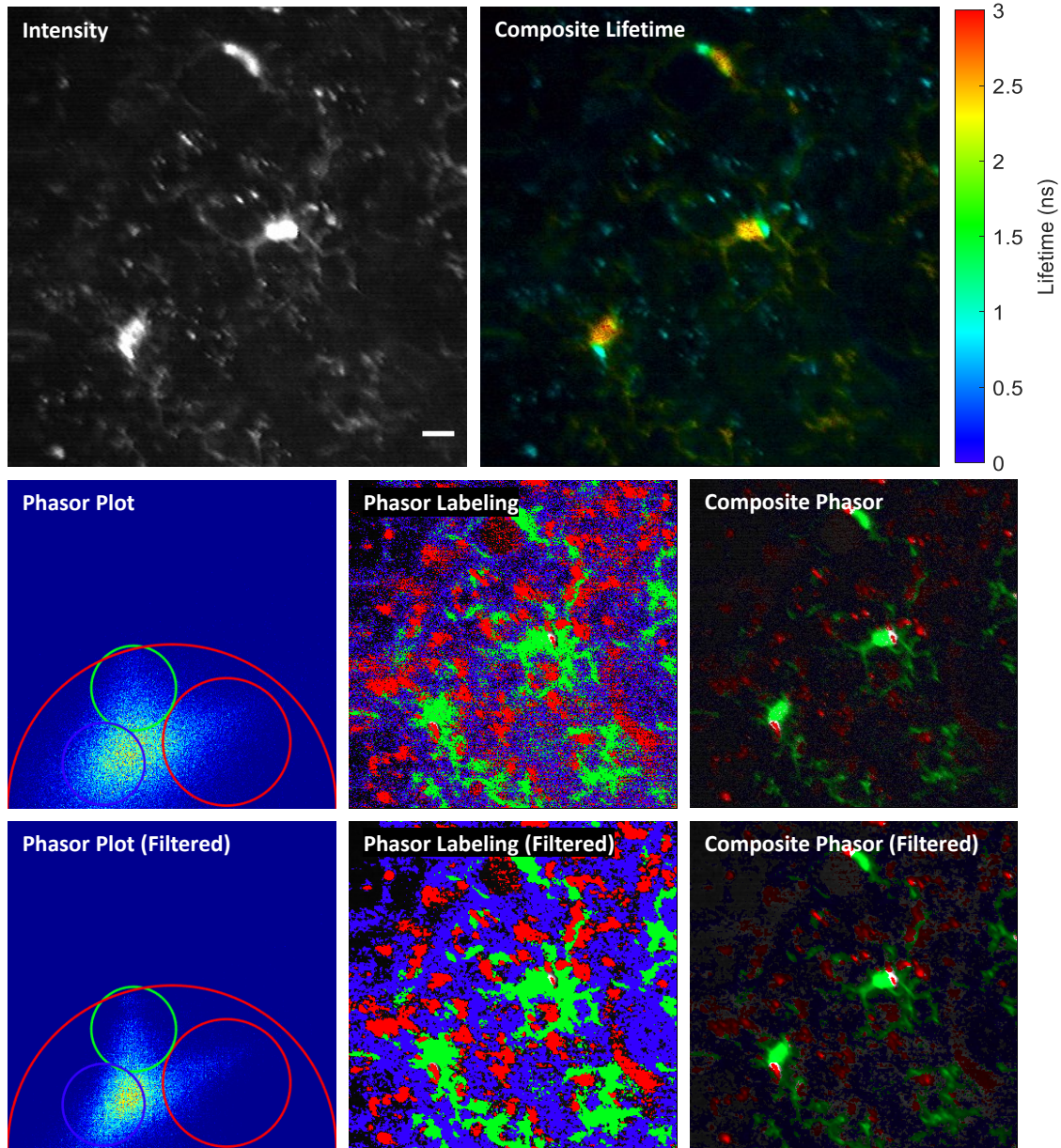


Figure 4. Images of live mouse brain (Cx3cr1-GFP/+) acquired with a PM-FLIM microscope.

Figure 3 shows the *ex vivo* PM-FLIM images of fixed BPAE cells. Here, in addition to intensity, composite lifetime, and phasor-related images, G, S, and lifetime images of gray scale are shown to illustrate the procedures of PM-FLIM. One can see the clear separation of cell mitochondria, F-actin, and nuclei by lifetime differences and phasor labeling. We also demonstrated *in vivo* fluorescence lifetime and phasor imaging on live mouse brain [Fig. 4] and live zebrafish embryo [Fig. 5]. In Fig. 4, the differences in microenvironments in the mouse brain, specifically, microglia, can be recognized by different lifetime values and phasor labels. In Fig. 5, different lifetime values and phasor labels represent different microenvironments surrounding the zebrafish spinal cord. Finally, 3D fluorescence lifetime and phasor labeling images of a live zebrafish embryo are shown in Fig. 6. Regardless of the samples or whether the images are acquired in 2D or 3D, the fluorescence lifetime and phasor labeling images can assist differentiating various cell or tissue structures that can not be separated by conventional intensity images. In particular, phasor plots and labeling, due to their versatility, are especially useful to separate the

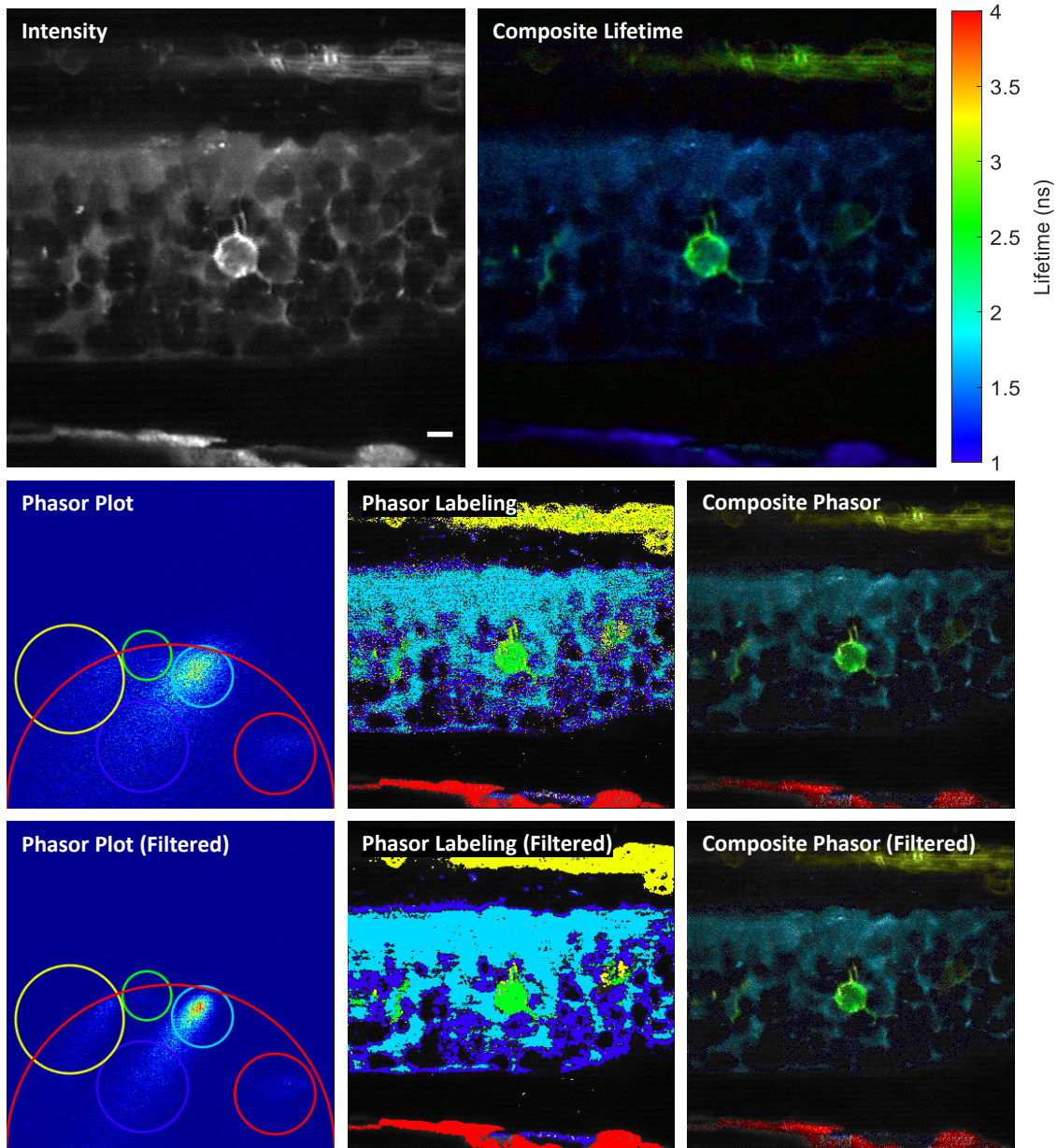


Figure 5. PM-FLIM images of live EGFP labeled Tg(sox10:megfp) zebrafish at 2 days post fertilization.

structures that can not be separated even by fluorescence lifetime images.

#### 4. CONCLUSION

We have proposed and demonstrated PM-FLIM, a novel MPM-FD-FLIM system capable of generating 3D fluorescence lifetime images in deep scattering tissues. The imaging speed of FLIM was improved using a RF analog signal processing technique termed phase multiplexing. Due to the multiplexing and analog signal processing, 3D fluorescence lifetime, phasor plots, and intensity images can be acquired simultaneously, with no additional time required for FLIM measurements. We have shown that this system allows for easy generation of phasor plots that can address multi-exponential fluorescence decay problems as well as exhibit the dynamics of the fluorophores being investigated. Finally, using a sensorless adaptive optics setup with a deformable mirror,

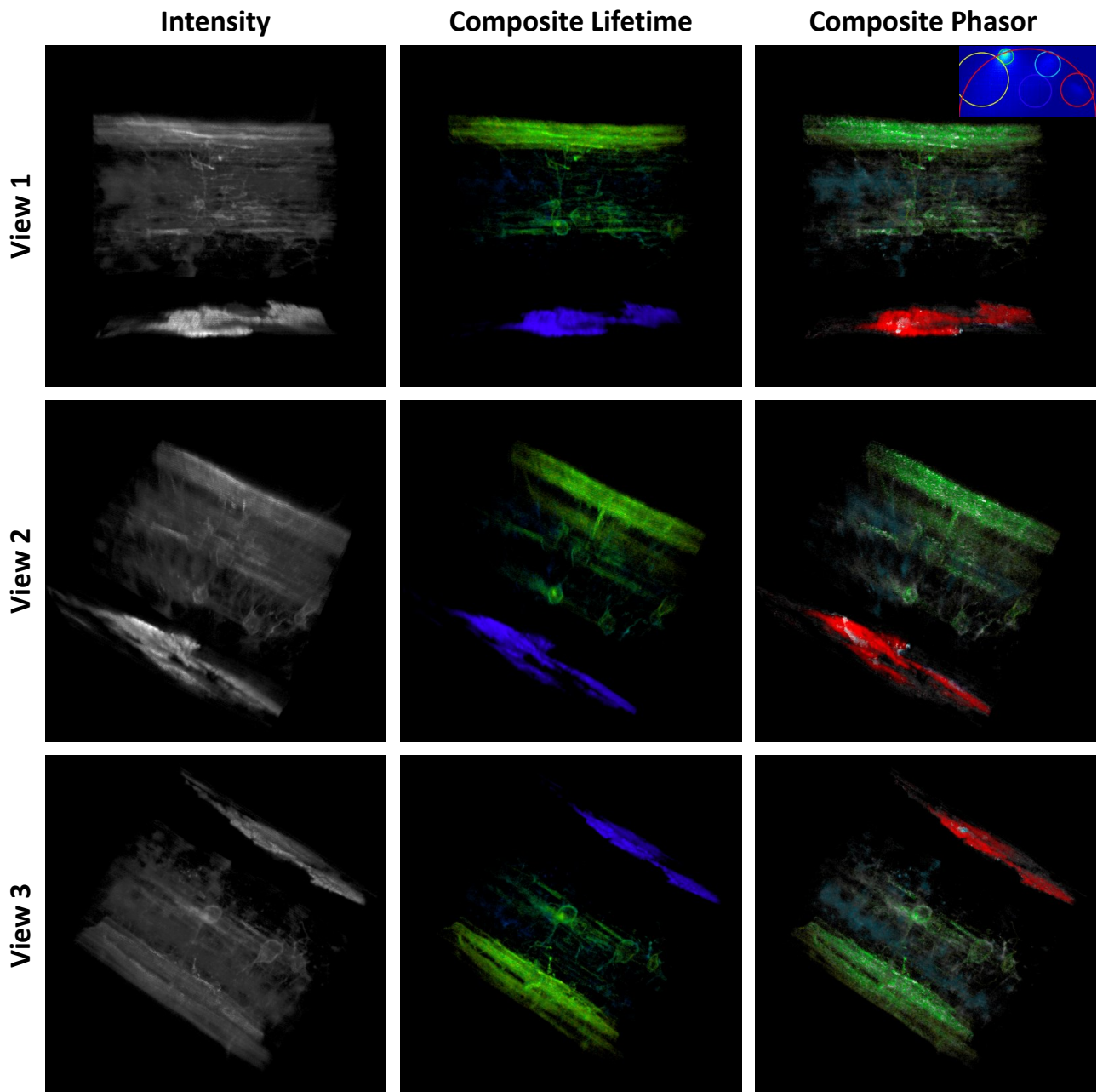


Figure 6. 3D fluorescence intensity, lifetime, and phasor labeled volumes of live zebrafish embryo acquired with a PM-FLIM microscope. Three different viewing angles are presented to help visualize the 3D structures. The difference in lifetime and phasor labels can be clearly observed in the 3D volumes.

we have demonstrated 3D lifetime images and phasor plots *in vivo* in deep scattering animal models, including live mouse brain and zebrafish embryo.

### ACKNOWLEDGMENTS

This work was supported by the University of Notre Dame, the Berry Family Foundation Graduate Fellowship of Advanced Diagnostics & Therapeutics (AD&T) (YZ), the National Science Foundation under Grant No. CBET-1554516 (SSH), NIH R01 CA194697 (SZ), NIH R01 CA222405 (SZ), the Elizabeth and Michael Gallagher Family

(CJS), and the Alfred P. Sloan Foundation (CJS). YZ would also like to acknowledge the support from a travel grant from the Harper Cancer Research Institute, University of Notre Dame.

## REFERENCES

- [1] Philip, J. and Carlsson, K., “Theoretical investigation of the signal-to-noise ratio in fluorescence lifetime imaging,” *J. Opt. Soc. Am. A* **20**(2), 368–379 (2003).
- [2] Li, D.-U., Arlt, J., Richardson, J., Walker, R., Buts, A., Stoppa, D., Charbon, E., and Henderson, R., “Real-time fluorescence lifetime imaging system with a  $32 \times 32$   $0.13 \mu\text{m}$  CMOS low dark-count single-photon avalanche diode array,” *Opt. Express* **18**(10), 10257–10269 (2010).
- [3] Khan, A. A., Fullerton-Shirey, S. K., and Howard, S. S., “Easily prepared ruthenium-complex nanomicelle probes for two-photon quantitative imaging of oxygen in aqueous media,” *RSC Adv.* **5**(1), 291–300 (2015).
- [4] Sakadžić, S., Roussakis, E., Yaseen, M. A., Mandeville, E. T., Srinivasan, V. J., Arai, K., Ruvinskaya, S., Devor, A., Lo, E. H., Vinogradov, S. A., and Boas, D. A., “Two-photon high-resolution measurement of partial pressure of oxygen in cerebral vasculature and tissue,” *Nat. Methods* **7**(9), 755–759 (2010).
- [5] Lecoq, J., Parpaleix, A., Roussakis, E., Ducros, M., Houssen, Y. G., Vinogradov, S. A., and Charpak, S., “Simultaneous two-photon imaging of oxygen and blood flow in deep cerebral vessels,” *Nat. Med.* **17**(7), 893–898 (2011).
- [6] Yaseen, M. A., Sakadžić, S., Wu, W., Becker, W., Kasischke, K. A., and Boas, D. A., “In vivo imaging of cerebral energy metabolism with two-photon fluorescence lifetime microscopy of NADH,” *Biomed. Opt. Express* **4**(2), 307–321 (2013).
- [7] Howard, S. S., Straub, A., Horton, N. G., Kobat, D., and Xu, C., “Frequency-multiplexed in vivo multiphoton phosphorescence lifetime microscopy,” *Nat. Photonics* **7**, 33–37 (dec 2012).
- [8] Zhang, Y., Khan, A. A., Vigil, G. D., and Howard, S. S., “Super-sensitivity multiphoton frequency-domain fluorescence lifetime imaging microscopy,” *Opt. Express* **24**, 20862–20867 (sep 2016).
- [9] Denk, W., Strickler, J. H., and Webb, W. W., “Two-photon laser scanning fluorescence microscopy,” *Science* **248**(4951), 73–76 (1990).
- [10] Zipfel, W. R., Williams, R. M., and Webb, W. W., “Nonlinear magic: multiphoton microscopy in the biosciences,” *Nat. Biotechnol.* **21**, 1369–1377 (Nov. 2003).
- [11] Hoover, E. E. and Squier, J. A., “Advances in multiphoton microscopy technology,” *Nat. Photonics* **7**, 93–101 (Jan. 2013).
- [12] Kumar, S., Dunsby, C., Beule, P. A. A. D., Owen, D. M., Anand, U., Lanigan, P. M. P., Benninger, R. K. P., Davis, D. M., Neil, M. A. A., Anand, P., Benham, C., Naylor, A., and French, P. M. W., “Multifocal multiphoton excitation and time correlated single photon counting detection for 3-D fluorescence lifetime imaging,” *Opt. Express* **15**(20), 12548–12561 (2007).
- [13] Becker, W., “Fluorescence lifetime imaging - techniques and applications,” *J. Microsc.* **247**, 119–136 (aug 2012).
- [14] Zhang, Y., Vigil, G. D., Cao, L., Khan, A. A., Benirschke, D., Ahmed, T., Fay, P., and Howard, S. S., “Saturation-compensated measurements for fluorescence lifetime imaging microscopy,” *Opt. Lett.* **42**, 155–158 (jan 2017).
- [15] Hato, T., Winfree, S., Day, R., Sandoval, R. M., Molitoris, B. A., Yoder, M. C., Wiggins, R. C., Zheng, Y., Dunn, K. W., and Dagher, P. C., “Two-photon intravital fluorescence lifetime imaging of the kidney reveals cell-type specific metabolic signatures,” *J. Am. Soc. Nephrol.* **28**, 2420–2430 (aug 2017).
- [16] Zhang, Y., Khan, A. A., Vigil, G. D., and Howard, S. S., “Investigation of signal-to-noise ratio in frequency-domain multiphoton fluorescence lifetime imaging microscopy,” *J. Opt. Soc. Am. A* **33**(7), B1–B11 (2016).
- [17] Zhang, Y., Benirschke, D., Abdalsalam, O., and Howard, S. S., “Generalized stepwise optical saturation enables super-resolution fluorescence lifetime imaging microscopy,” *Biomed. Opt. Express* **9**, 4077–4093 (sep 2018).
- [18] Stringari, C., Cinquin, A., Cinquin, O., Digman, M. A., Donovan, P. J., and Gratton, E., “Phasor approach to fluorescence lifetime microscopy distinguishes different metabolic states of germ cells in a live tissue,” *Proc. Natl. Acad. Sci. USA* **108**, 13582–13587 (aug 2011).
- [19] Berberan-Santos, M. N., “Phasor plots of luminescence decay functions,” *Chem. Phys.* **449**, 23–33 (2015).

- [20] Ranjit, S., Malacrida, L., Jameson, D. M., and Gratton, E., “Fit-free analysis of fluorescence lifetime imaging data using the phasor approach,” *Nat. Protoc.* **13**, 1979–2004 (sep 2018).
- [21] Palczewska, G., Dong, Z., Golczak, M., Hunter, J. J., Williams, D. R., Alexander, N. S., and Palczewski, K., “Noninvasive two-photon microscopy imaging of mouse retina and retinal pigment epithelium through the pupil of the eye,” *Nat. Med.* **20**(7), 785–789 (2014).